Astron. Astrophys. 348, 621–626 (1999)

ASTRONOMY AND ASTROPHYSICS

Fine structure in sunspots

III. Penumbral grains

M. Sobotka[1], **P.N. Brandt**[2], **and G.W. Simon**[3]

[1] Astronomical Institute, Academy of Sciences of the Czech Republic, CZ-25165 Ondřejov, Czech Republic
[2] Kiepenheuer-Institut, D-79104 Freiburg, Germany
[3] Air Force Research Laboratory and National Solar Observatory, Sunspot, NM 88349, USA

Received 26 February 1999 / Accepted 7 June 1999

Abstract. The properties of penumbral grains (PGs) in a medium-size sunspot are studied from a 4.5 hour observation series acquired on 5 June 1993 at the Swedish Vacuum Solar Telescope, La Palma. The application of an image segmentation procedure and a feature tracking algorithm on a movie of 360 frames yields proper motions, intensities, and lifetimes for a set of 469 PGs. Almost 3/4 of the PGs move toward the umbra and more than 1/4 toward the photosphere. There appears to be a dividing line (DL) in the penumbra, approximately 0.7 of the distance from the umbra to the photosphere, such that most PGs outside this line move toward the photosphere, and those inside move toward the umbra. For inward moving PGs we find a typical proper motion speed of 0.4 km s^{-1} and a median lifetime of 29 minutes, for outward moving ones 0.5 km s^{-1} and 22 minutes. The average speed of inward moving PGs increases with distance from the umbra with a maximum near the DL. Outward moving PGs have maximum speed near the outer penumbral boundary. The measured instantaneous velocities of individual PGs show only partial agreement with theoretical model predictions. We find much shorter lifetimes than earlier authors, and no pronounced dependence of lifetime on position in the penumbra. We discuss possible reasons for the disagreement with previous results.

Key words: Sun: sunspots – convection

1. Introduction

The penumbra of a sunspot consists of bright filaments separated by dark fibrils. Bright filaments are, in fact, chains of elongated bright features called penumbral grains (PGs, Muller 1973a,b). They have comet-like shapes with "heads" pointing towards the umbra. Their width is $0\farcs4$ on average, and their length ranges from $0\farcs4$ to more than $2''$. The brightness of the "heads" approaches that of the photosphere. PGs have not been studied by many authors because successful observations require an extended period of excellent seeing.

Send offprint requests to: M. Sobotka (msobotka@asu.cas.cz)

Schröter (1962) noted that "Bright knots as seen in the penumbral filaments show ... a systematic motion (1–2 km/s) away from the center of the spot." Muller (1973a) used an excellent series of 34 white-light photographs, taken at Pic du Midi and covering an interval of 3 hours, to identify and track visually 220 PGs in order to determine both velocities and lifetimes as functions of position within the penumbra. He claimed that PGs moved toward the umbra; their horizontal speed was maximum (0.5 km s^{-1}) at the penumbra-umbra (P/U) border and zero at the penumbra-photosphere (P/Ph) boundary. The lifetimes were about 3 hours in the middle part of the penumbra, and 50 and 40 minutes in the inner and outer parts, respectively. Tönjes & Wöhl (1982), using a similar method, in general confirmed the results of Muller but found lower horizontal velocities with a maximum of 0.33 km s^{-1} located in the middle penumbra. Lifetimes ranged from 1 to 3 hours.

The horizontal motions in penumbrae can be measured using local correlation tracking (LCT, November & Simon 1988). Because of LCT's inherently poor spatial resolution (typically $1''$–$2''$), and its inability to distinguish between motions of bright or dark features, it is not clear that LCT of a sunspot penumbra is tracking solely PGs, or also other penumbral features. Wang & Zirin (1992) applied LCT to series (duration 2–3 hours) of digitized video images of five sunspots. In four cases they observed that "both bright grains and dark fibrils in the inner part of the penumbra move toward the umbra at a speed of about 0.5 km s^{-1}" and "the elements in the outer part of the penumbra move outward at about the same speed as the inflow." In one case the inflow occurred over the whole penumbra. Also applying LCT, Denker (1998) reported that a line of positive divergence divides the penumbra, implying opposite directions of motion in the inner and outer parts.

The average observed brightness of PGs ($\lambda = 550$ nm) and dark spaces between them is 0.95 and 0.60 of the mean photospheric intensity ($I_{\rm phot}$), respectively (Muller 1973b, Collados et al. 1988). Recently, Sütterlin & Wiehr (1998) presented a temperature map derived from speckle-reconstructed three-color photometry of a large sunspot. The sunspot penumbra shows typical spatial temperature fluctuations of 700 K. The mean temperature of PGs is about 6250 K, hotter by 100 K than

the mean photosphere. Dark penumbral fibrils have an average temperature of 5650 K, corresponding to an intensity of 0.64 $I_{\rm phot}$.

A theoretical explanation for PGs has been suggested by Schlichenmaier et al. (1998a,b). According to their model, a PG is the intersection (footpoint) of an inclined thin magnetic flux tube with the visible surface. Hot sub-photospheric plasma flows upward along this tube. As the flux tube rises, its inclination decreases, so that the footpoint exhibits a horizontal motion toward the umbra. The model predicts a gradual decrease of horizontal velocity from 2 km s^{-1} at the beginning, to 0.1 km s^{-1} at the end, of a PG's lifetime. Bright filaments are interpreted as dimmer and thinner tails of PGs. Their width is very small, only 50 km. The extreme narrowness of penumbral filaments was confirmed by Sánchez Almeida & Bonet (1998) who found that the spatial spectrum of penumbral intensity fluctuations, corrected for the instrumental modulation transfer function, was flat up to the highest observable spatial frequency. This implies that the true structure of penumbral filaments has not yet been resolved.

In 1993 an 11-hour time series of high-resolution white-light images of solar granulation was obtained by Simon et al. (1994). A medium-size sunspot was present in the field of view for about 4.5 hours. Sobotka et al. (1997a,b – Papers I and II of this series) analyzed temporal variations of sunspot fine structure in the central umbral core, and applied a feature tracking algorithm to umbral dots. We now use this algorithm to measure proper motion, brightness, and lifetime of PGs in the penumbra of this sunspot. Preliminary results have been published by Sobotka et al. (1999). We have made substantial improvements in the algorithm, and here present our revised results. We hope these will spur refinement of theoretical models, and stimulate further discussion of the earlier measurements.

2. Observations and data analysis

The observations, data reduction, basic ideas on the identification and tracking algorithms, determination of image sharpness, and discussion of stray light effects have been thoroughly described in Paper I. Here we only give a brief summary of facts and methods that are common to both Paper I and this work, but present more detailed information about specific changes and problems related to the penumbral data analysis.

The sunspot NOAA 7519 was observed at heliographic position N05, E15 on 5 June 1993 with the Swedish Vacuum Solar Telescope (SVST, aperture 50 cm) at La Palma, Canary Islands (Simon et al. 1994). This slowly evolving spot reached maximum area on the date of observation. A Kodak Megaplus Model 1.4 CCD camera, in connection with a fast real-time frame selection system (working at approx 3.5 frames/s), was used to sample white light solar images at $\lambda = 4680 \pm 50$ Å. The image scale was $0\farcs125$ per pixel. Due to image rotation during the 11-hour time series, the sunspot was visible only for 4 hours 26 minutes, from 09:54 to 14:20 UT, during which we obtained 760 frames. After correcting for dark current, flat field, rotation, transparency, and exposure variations we reduced the field of view to 288×288 pixels, or $36'' \times 36''$, centered on the spot. The frames were registered, corrected for instrumental profile, and destretched, to minimize seeing distortions. From these we selected 360 frames with rms granulation contrast higher than 7%, covering almost regularly the whole time period. The selected frames were then interpolated in time to obtain a time series with a constant lag of 44.5 s. Residual seeing-induced jitter which impeded the tracking of PGs in time was removed by $k-\omega$ (subsonic) filtering. The cutoff phase velocity of the filter was set at 3 km s^{-1}. For further analysis we selected three subfields of the sunspot that showed regular penumbrae.

To isolate PGs in the subfields we applied a geometrical mask to exclude light bridges, eliminated umbral dots by setting the minimum intenstity of bright features to 0.8 $I_{\rm phot}$, and removed photospheric features located outside the P/Ph boundary. After this preparatory phase we tested several segmentation procedures to separate PGs from the rest of the penumbra. This task was more complicated than in the case of umbral dots due to the complex and fast-changing penumbral intensity structure.

We adopted a procedure similar to that described in Paper I: For each frame a differential image was computed by subtracting a smoothed ($0\farcs875 \times 0\farcs875$ boxcar) image from the original one. From this differential image we computed a binary mask, setting pixel values higher than a certain threshold to 1 and the rest to 0. The threshold was defined as a linear function of the image sharpness, computed for each frame with the Roberts gradient operator (see Paper I), such that its values were 0.06, 0.04, and 0.03 in the best, average, and worst frames, respectively. The original image was then multiplied by this mask, producing a segmented image.

From the images we produced a time series of variable-threshold segmented frames. A feature tracking algorithm, described in Paper I, was applied to this series to follow each PG in time. To be called a PG, each feature had to:

(a) be larger than 1 pixel on each frame;
(b) overlap in at least 1 pixel on subsequent frames;
(c) have a maximum interruption of 3 frames;
(d) have a lifetime of at least 3 minutes;
(e) have a mean area over its lifetime of at least 9 pixels.

This procedure yielded a set of 1027 PGs. For each of these we tracked the locus and value of maximum intensity at each time step. Lifetimes were derived from the number of frames in which the objects were present. Time-averaged proper motion velocities were calculated using linear least-squares fits to the positions. Since the accuracy of velocity determinations increases with the number of frames in which the PG is present, we chose for analysis 649 PGs with lifetimes longer than 12 minutes. In this new set, the standard deviation is about 0.05 km s^{-1}.

In the last step of the data analysis we checked visually the trajectories of these 649 PGs to eliminate spurious objects and mistakes in feature tracking. We discarded all features that showed:

(1) discontinuities in position or strong bends/breaks in the trajectory (caused by spurious coincidences of independent objects);

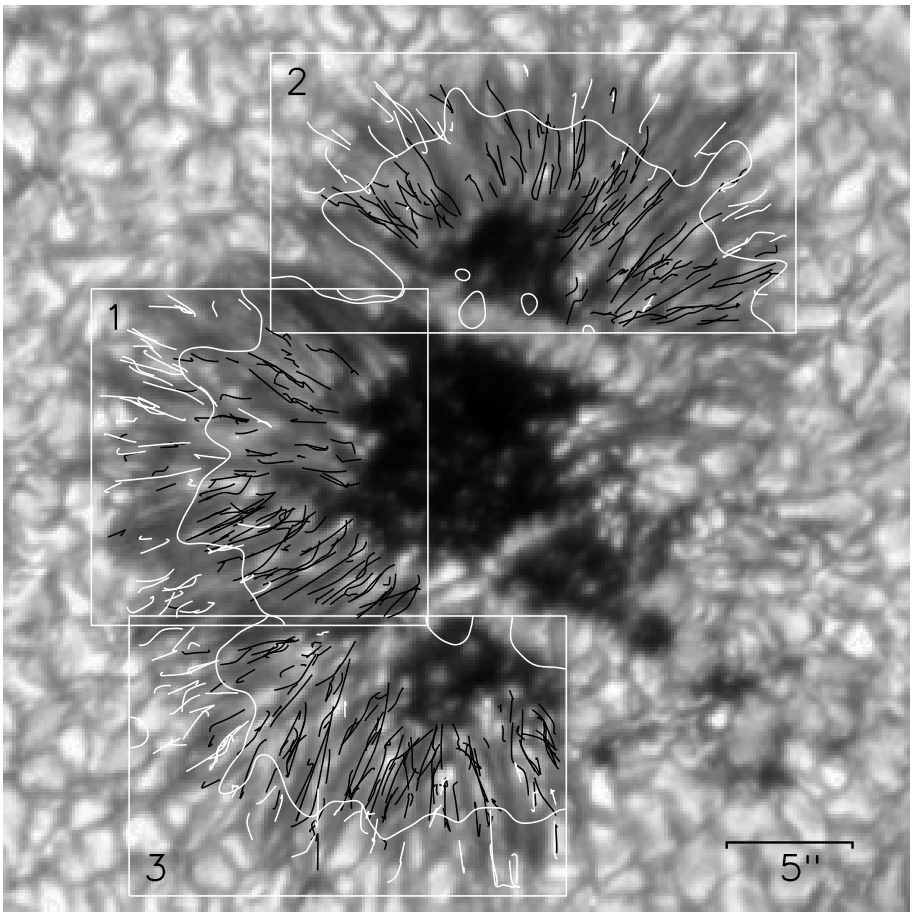

Fig. 1. Trajectories of INW (black) and OUT (white) PGs in subfields 1, 2, and 3. The white contour lines divide regions of inward and outward motions of both bright and dark penumbral features as derived by LCT. The underlying image is one of the best frames in the middle of the series.

(2) repeated back-and-forth motions (wrong tracking of poorly defined large features);
(3) stationary objects at the P/U or P/Ph boundary (border effects).

After this visual consistency check we obtained a final sample of 469 PGs whose proper motions, intensities, and lifetimes were investigated.

3. Results

3.1. Proper motions of penumbral grains

The trajectories of PGs were determined from the positions tracked in time and smoothed by cubic splines. Of the 469 PGs, 341 (almost 3/4) move inward toward the umbra. We label them INW. More than 1/4 (128 PGs) move outward toward the photosphere. We call them OUT. There appears to be a *dividing line* (DL) in the penumbra, approximately 0.7 of the distance from the umbra to the photosphere. Outside the DL most PGs (75 %) are of type OUT; inside most (89 %) are INW. This phenomenon is illustrated in Fig. 1, in which we show trajectories of the INW and OUT PGs as black and white lines, respectively. The lengths of trajectories are in the range $0\farcs3$–$4\farcs8$ for INW and $0\farcs3$–$3\farcs5$ for OUT PGs. The mean values are $1\farcs4$ and $1\farcs1$, respectively, in a penumbra of average width $8\farcs7$. We did not observe any PG crossing the whole penumbra. Some INW PGs moved into the umbra but tracking was terminated when their brightness decreased below the 0.8 $I_{\rm phot}$ limit – such features are not the subject of this study.

In addition to tracking individual PGs we applied an LCT algorithm with a tracking window of $1''$. The flow maps were then averaged over the whole time series. We obtain the same results as reported by Wang & Zirin (1992): Both bright and dark penumbral features move inward in the inner part of the penumbra and outward in the outer part. The boundary between inward and outward motions, defined as the line connecting the LCT zero-velocity points, is plotted in Fig. 1. It separates most trajectories of INW and OUT PGs and is located very close to the position of the DL that we would have chosen by eye (though such a hand-drawn line would not have had the convoluted shape of the contour line). This indicates a consistency between LCT flow maps and the motions of individual PGs as determined by feature tracking.

The histogram of time-averaged proper motion speeds is shown in Fig. 2 (left). Speeds for INW PGs range from 0.0 to 2.0 $\mathrm{km\,s^{-1}}$ with a maximum around 0.3–0.4 $\mathrm{km\,s^{-1}}$ and a median of 0.43 $\mathrm{km\,s^{-1}}$. Speeds of the OUT PGs are in the same range but the maximum is around 0.5–0.6 $\mathrm{km\,s^{-1}}$ and the median is 0.53 $\mathrm{km\,s^{-1}}$. These values do not differ substantially from those measured by Muller (1973a) and Tönjes & Wöhl (1982).

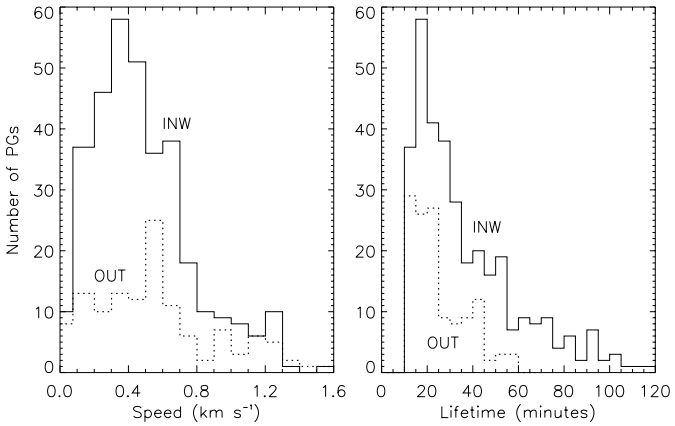

Fig. 2. *Left:* Histogram of time-averaged speeds of PGs. Solid line (INW), dotted line (OUT). *Right:* Histogram of PG lifetimes (lower limit was set to 12 minutes).

To study the dependence of time-averaged velocities on position, we divided the penumbra into 10 bins, each covering 0.1 of the relative distance from the P/U (position 0.0) to the P/Ph boundary (position 1.0). Velocities of all PGs whose time-averaged positions fell into a given bin were averaged. The results are plotted in Fig. 3 (top) together with 1σ error bars which characterize the scatter of individual values.

For the INW PGs speeds increase from about $0.4\,\mathrm{km\,s^{-1}}$ at the P/U boundary to a maximum of $0.75\,\mathrm{km\,s^{-1}}$ at the relative distance 0.7–0.8 (just outside the DL) and then drop to about $0.5\,\mathrm{km\,s^{-1}}$ near the P/Ph border. Speeds of the OUT PGs show a strong increase from $0.2\,\mathrm{km\,s^{-1}}$ in the middle penumbra (position 0.4–0.5) to a maximum of $0.7\,\mathrm{km\,s^{-1}}$ near the P/Ph boundary. Note, however, that the numbers of OUT PGs at positions less than 0.6, and of INW PGs at positions greater than 0.8, are very small, as can be seen in Fig. 3.

The observed dependence of INW speeds on relative position in the penumbra is qualitatively similar to the prediction given in the model by Schlichenmaier et al. (1998b, Fig. 7). To compare PG motions in detail with the results of the model, we calculated instantaneous velocities of each PG as derivatives of positions smoothed by cubic splines. Individual velocity curves, showing variations of speed with time, were divided into five types:

– = constant speed
/ = acceleration
\ = deceleration
∩ = acceleration, then deceleration
∪ = deceleration, then acceleration

Numbers of INW and OUT PGs belonging to the different speed types are summarized in Table 1. For INW PGs, decelerating (35 %) and accelerating (30 %) types are most common, while 33 % have more complex behavior ("∩" and "∪"). Only decreasing of INW speed with time, i.e. type "\", agrees with the model prediction. About 1/3 of OUT PGs increase their speed with time. The maximum instantaneous speed for both INW and OUT PGs is in the range 2–3 $\mathrm{km\,s^{-1}}$, matching the value predicted by the model.

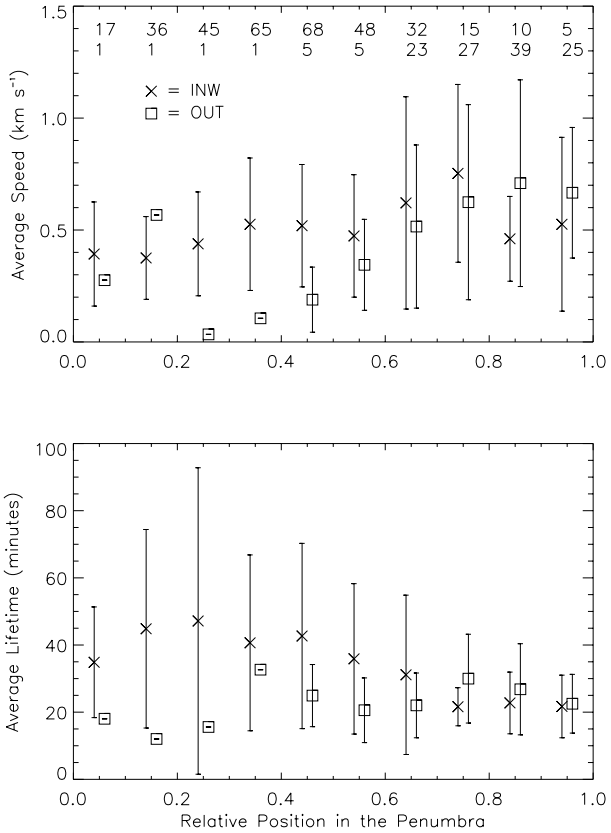

Fig. 3. *Top:* Average speed of PGs as function of their relative position in the penumbra. INW PGs are represented by ×, OUT PGs by □. Position is 0.0 at umbra, 1.0 at photosphere. The bars indicate a scatter of $\pm\ 1\sigma$. Numbers of INW (OUT) PGs in each bin are displayed in the upper (lower) row. *Bottom:* Average lifetime of PGs as function of their relative position in the penumbra.

Table 1. Numbers of PGs by speed type

Type	INW	%	OUT	%
–	8	2	2	2
/	101	30	44	34
\	118	35	35	27
∩	49	14	24	19
∪	65	19	23	18
Totals	341	100	128	100

3.2. Photometric characteristics of penumbral grains

As mentioned earlier, we obtained the brightness maximum of each PG at each time step as one of the outputs of the feature-tracking routine. The temporal intensity fluctuations, characterized by $\sigma = 0.05\ I_{\mathrm{phot}}$, are small. The time-averaged intensities are in the range 0.84–1.10 I_{phot} for both INW and OUT PGs, but OUT PGs are brighter on average (0.96 I_{phot}) than the INW ones (0.94 I_{phot}). The intensities do not depend on relative dis-

tance from the umbra. They are uncorrelated with the speeds or lifetimes of PGs.

We used the best frame of the series to do complementary visual measurements of lengths, widths, and contrasts of 56 PGs. The lengths lie in a broad range from $0\farcs6$ to $3\farcs7$; the average value is $1\farcs7$. The mean and standard deviation of widths measured across the "heads" of PGs are $0\farcs5 \pm 0\farcs1$. The intensity of the "heads" is typically 0.94 $I_{\rm phot}$, 1.4 times brighter on average than adjacent dark fibrils. Since the intensities are influenced by scattered light, the real contrast is probably higher.

Balthasar et al. (1996) reported that the mean white-light image of a penumbra averaged over nearly 2 hours still showed radial structures. We confirm this result. Averaging frames over our 4.5 hour series we find a filamentary structure in the penumbra (of course without PGs, which have disappeared due to time-smoothing) with rms contrast of 7 %. For comparison, the penumbral rms contrast in our best frames is about 12 %. This remarkable persistence of high contrast over many hours must be due to the stability of the magnetic field configuration. This stability causes the paths of many individual PGs to follow nearly identical trajectories.

3.3. Lifetimes of penumbral grains

Since lifetimes are derived from the number of frames in which individual PGs are observed, histories of some PGs will be cut off at the beginning or end of the time series. However, this effect is small, because most of the lifetimes are substantially shorter than the duration of the series. We show in Fig. 2 (right) a histogram of lifetimes for the 341 INW and 128 OUT PGs that passed the visual consistency check. For the INW PGS the maximum lifetime is almost four hours (231 minutes) but only 17 % live longer than 1 hour; the median and mean lifetimes are 29 and 39 minutes, respectively. The OUT PGs live shorter than the INW ones: the maximum, median, and mean lifetimes are 59, 22, and 25 minutes, respectively.

The number of PGs increases with decreasing lifetime t to the limit of 12 minutes. (Recall that in Sect. 2 we had set the minimum lifetime of visually checked PGs to this value.) Of course, we expect a large population of PGs to have $t < 12$ minutes, and try to estimate this number as follows: Of the total sample of 1027 PGs, 378 lived less than 12 minutes. Assuming the same fraction of PGs that have to be discarded (0.28) and relative numbers of INW and OUT PGs (0.73 and 0.27) as in the case of the $t > 12$ minute population, we get about 198 (74) "good" short-lived INW (OUT) PGs. Adopting 7 minutes for the average lifetime of PGs with $t < 12$ minutes, as derived from the statistics of the unchecked sample, we extrapolate the median and mean lifetimes for all INW (OUT) PGs to about 17 and 27 (15 and 19) minutes, respectively.

The average lifetime of PGs with $t > 12$ minutes as function of position in the penumbra is shown in Fig. 3 (bottom). The mean lifetime of INW PGs rises from 35 minutes for those at the P/U boundary to a maximum of 47 minutes at the relative position 0.2–0.3, and then decreases to 22 minutes at positions 0.7–1.0 between the DL and the P/Ph border. The lifetime of OUT PGs exhibits little trend as function of position, and has a mean value about 25 minutes. The average lifetime of INW PGs that show deceleration at the beginning of their existence (speed types "$\backslash$" and "$\cup$") is longer by a factor of 1.2 than that of the other INW PGs. For OUT PGs we observe no relation between lifetime and speed type.

In summary, while we agree with Muller (1973a) that the average lifetime of INW PGs in the inner part of the penumbra is larger than for those near the P/Ph boundary, we do not see the pronounced dependence of lifetime on penumbral position reported by Muller (1973a) and Tönjes & Wöhl (1982). More significantly, the lifetimes we measure are only about one-fourth those of the earlier measurements.

4. Discussion

The average PG velocities that we measure are in reasonably good agreement with those of Muller (1973a) and Tönjes & Wöhl (1982), but the character is very different. Whereas they find almost exclusively INW motions, we find both INW and OUT, with a strong dependence on position in the penumbra as described in Sect. 3.1. Although Muller (1973a) states in his summary that all motions are INW, careful examination of his Fig. 3 shows that he actually found a few OUT PGs at penumbral positions 0.25–0.80, and more OUT than INW PGs in the outermost penumbra (positions 0.8–1.0). Thus the qualitative difference in our results may not be as large as it first appears. All three of these observations show velocities far smaller than those of Schröter (1962).

The LCT flow maps calculated by Wang & Zirin (1992) show that both bright and dark penumbral structures in the inner part of the penumbra move toward the umbra, and those in the outer part move outward. This was observed in four of five sunspots, but in one very young spot inflow occurred in the whole penumbra. Since we found in Sect. 3.1 that the LCT flows seem to be consistent with the motions of individual PGs, we can infer that a part of the discrepancy between our work and Muller's (1973a) may simply be the physical properties of the particular sunspots studied. Our spot was of medium size, in the maximum phase of evolution; Muller's was very large. The character of the motions may vary significantly as function of size, age, evolutionary stage (young, old, growing, decaying), and location (unipolar, leading, following, simple or complex group), etc. Thus it is likely that Muller (1973a) and we are both correct despite our disparate results.

On the other hand, the difference may, at least in part, lie in the methods of analysis and/or quality of the observational data. Muller (1998, private communication) believes that "investigations based on visual identifications are superior to investigations based on computer identifications, because they are more 'intelligent'; one can see the evolution of grains in more detail, understand better what happens and take some decisions; it is less sensitive to threshold effects, because the eyes can detect small contrasts." He acknowledges that his process "is tedious and time-consuming and might not be objective enough in the decisions." This last comment by Muller is the main reason

that we prefer computer identification of features. Even though the algorithms may occasionally make mistakes, they are completely objective in their decision-making. Also they are not subject to two biases inherent in visual identification; namely, the tendency of the eye-brain interaction to selectively prefer brighter (higher contrast) and larger features. The computer is ideally suited to performing tedious tasks; thus it selects far more features for analysis than the human analyst is physically or psychologically prepared to do.

With regard to the shorter lifetimes that we measure, we agree with Muller "that the difference in lifetime we find in our respective investigations is mainly due to the different time interval between frames and to different ways we identify the penumbral grains." Our time interval (44.5 s) is about eight times shorter than Muller's (1973a, 6 minutes). It is clear that with lower temporal resolution the mean lifetime increases, because short-lived objects do not appear in the statistics and false coincidences of independent objects are more probable. Our time series is also 50 % longer than Muller's, and this, in combination with our smaller time intervals, means that our statistics are significantly better than Muller's. Concerning the identification and tracking methods, we also suggest that the human eye-brain system, compared to the computer, is more likely to look for long-lived objects.

One unsolved mystery which should be pursued with other data sets is the comet-like shape of many PGs. Muller (1973a,b) says their "heads" point toward the umbra. We agree that INW PGs show this behavior. But why, then, do not the heads of OUT PGs point toward the photosphere? We find that the shapes of OUT PGs are less regular than those of INW – sometimes the heads point toward the photosphere, sometimes toward the umbra, sometimes there are no tails, and sometimes no heads.

Finally, what is a penumbral grain? Since it is bright, it must represent localized heating within a penumbral filament. Since we see PGs "move", do these moving brightenings indicate mass motion of hot material or are they only phase velocities of brightness fluctuations? Perhaps these bright features are the loci of the intersections with the photosphere of hot, rising, flux tubes as suggested by Schlichenmaier et al. (1998a,b). Except for a brief acceleration at the beginning of a PG's life, their model predicts inward phase motions that decelerate in time. Only 25 % of PGs observed by us move in this particular way. We hope that the numerical simulations can be refined to account for the interaction of several flux tubes, for repeated travelling of individual PGs along "preferred" trajectories (as shown by the persistent filamentary pattern in time-averaged images), and to explain both the inward and outward observed motions.

Acknowledgements. We especially thank Richard Muller for very helpful discussions and permission to quote his unpublished comments. We thank G. Scharmer for the opportunity to observe at the SVST, W. Wang and R. Kever for observational support, and M. Shand of DEC (Paris) for financial and technical assistance with the data acquisition system. The work of M.S. was accomplished under Grant A 3003903 by the Grant Agency of the Academy of Sciences of the Czech Republic (ASCR) and under the Key Project K1-003-601 of the ASCR. We gratefully acknowledge funding from the U.S. Air Force Office of Scientific Research for salary (G.W.S.) and travel support (P.N.B. and M.S.). The SVST is operated on the island of La Palma by the Royal Swedish Academy of Sciences at the Spanish Observatorio del Roque de los Muchachos of the Instituto de Astrofísica de Canarias.

References

Balthasar H., Schleicher H., Bendlin C., Volkmer R., 1996, A&A 315, 603
Collados M., del Toro Iniesta J.C., Vázquez M., 1988, A&A 195, 315
Denker C., 1998, Solar Phys. 180, 81
Muller R., 1973a, Solar Phys. 29, 55
Muller R., 1973b, Solar Phys. 32, 409
November L.J., Simon G.W., 1988, ApJ 333, 427
Sánchez Almeida J., Bonet J.A., 1998, ApJ 505, 1010
Schlichenmaier R., Jahn K., Schmidt H.U., 1998a, ApJ 493, L121
Schlichenmaier R., Jahn K., Schmidt H.U., 1998b, A&A 337, 897
Schröter E.H., 1962, Z. Astrophys. 56, 183
Simon G.W., Brandt P.N., November L.J., Scharmer G.B., Shine R.A., 1994, In: Rutten R.J., Schrijver C.J. (eds.) Solar Surface Magnetism. Kluwer, Dordrecht, p. 261
Sobotka M., Brandt P.N., Simon G.W., 1997a, A&A 328, 682
Sobotka M., Brandt P.N., Simon G.W., 1997b, A&A 328, 689
Sobotka M., Brandt P. N., Simon G. W., 1999, In: Rimmele T.R., Balasubramaniam K.S., Radick R.R. (eds.) High Resolution Solar Physics: Theory, Observations, and Techniques. ASP Conf. Ser., in press
Sütterlin P., Wiehr E., 1998, A&A 336, 367
Tönjes K., Wöhl H., 1982, Solar Phys. 75, 63
Wang H., Zirin H., 1992, Solar Phys. 140, 41